

Experimental measurement of water wave band gaps

Taek Seong Jeong, Jae-Eun Kim, Hae Yong Park, and In-Won Lee

Citation: *Appl. Phys. Lett.* **85**, 1645 (2004); doi: 10.1063/1.1787941

View online: <http://dx.doi.org/10.1063/1.1787941>

View Table of Contents: <http://apl.aip.org/resource/1/APPLAB/v85/i9>

Published by the [American Institute of Physics](#).

Additional information on *Appl. Phys. Lett.*

Journal Homepage: <http://apl.aip.org/>

Journal Information: http://apl.aip.org/about/about_the_journal

Top downloads: http://apl.aip.org/features/most_downloaded

Information for Authors: <http://apl.aip.org/authors>

ADVERTISEMENT



Goodfellow
metals • ceramics • polymers • composites
70,000 products
450 different materials
small quantities fast

www.goodfellowusa.com

Experimental measurement of water wave band gaps

Taek Seong Jeong, Jae-Eun Kim, and Hae Yong Park^{a)}

Department of Physics, Korea Advanced Institute of Science and Technology, Taejeon 305-701, Korea

In-Won Lee

Department of Civil Engineering, Korea Advanced Institute of Science and Technology, Taejeon 305-701, Korea

(Received 29 March 2004; accepted 29 June 2004)

We experimentally demonstrate the existence of water wave band gaps in finite two-dimensional periodic graphitic and triangular structures composed of vertical cylinders which stand on the bottom of the water tank and project out of the water surface. The experimental data agree fairly well with the numerical simulations obtained from the multiple scattering method. The experimental evidence of water wave band gaps suggests that two-dimensional periodic structures of vertically oriented solid cylinders constitute a much better solution for the problem of coastal erosion. © 2004 American Institute of Physics. [DOI: 10.1063/1.1787941]

During the last decade, intensive attention has been focused on artificial crystals, which are spatially periodic structures composed of different elements.^{1,2} Multiple scattering from such structures prevents the propagation of waves in them over a wide range of frequencies, leading to a control over the wave propagation to suit a desired purpose. For example, photonic crystals, constructed with periodic dielectric composites, have photonic band gaps. The concept of photonic band gaps for electromagnetic waves in artificial crystals has been extended to other types of waves, such as acoustic waves^{3,4} and water waves.⁵⁻⁹ In particular, numerical simulations have shown that finite two-dimensional (2D) periodic structures, with water wave band gaps (WWBGs), are good candidates for coastal protection.⁹ However, the lack of experimental evidence for WWBGs has rendered this suggestion unreliable so far. In this letter, we confirm the existence of WWBGs experimentally by measuring the transmission spectra of water waves in 2D periodic structures on a laboratory scale and compare the experimental results with numerical calculations.

For a numerical simulation of the transmission properties of water waves through artificial crystals, we use the multiple-scattering method.¹⁰ We consider the linear interaction of monochromatic water waves with fixed vertically oriented cylinders with the top of the cylinders projecting out of the water surface. In the analysis, both a Cartesian coordinate system (x, y, z) as well as a cylindrical coordinate system (r, θ, z) , are used with the z axis pointing vertically upwards and $z=0$ defining the mean water surface. In the linear assumption, the water waves may be characterized by a velocity potential $\Phi(x, y, z, t)$. Assuming time-harmonic waves, with angular frequency ω , the velocity potential can be written as

$$\Phi(x, y, z, t) = \text{Re}[\phi(x, y) \cosh k(z+h) e^{-i\omega t}], \quad (1)$$

where k is the wave number. The dispersion relation for water waves is $\omega^2 = (gk + \tau_0 k^3 / \rho_0) \tanh(kh)$, where h is the depth of the water, τ_0 the surface tension (0.073 N/m), and ρ_0 the density of water (1 g/cm³), respectively. We express the total velocity potential as a sum of potentials for the incident and

scattered waves from each cylinder as follows:

$$\phi = \phi_I + \sum_{j=1}^N \phi_S, \quad (2)$$

where ϕ_I and ϕ_S represent the incident and scattered potentials, respectively. Each potential is further expanded in terms of the Fourier-Bessel functions. Under the no-flow conditions at solid boundaries, the boundary condition on the surface of each cylinder becomes $\partial\phi/\partial\mathbf{n}=0$, where \mathbf{n} is the vector normal to the surface of the cylinders. After some algebra, we can obtain an expression for the velocity potential from which an expression for the elevation η of the waves from the mean air-water surface may be obtained as

$$\eta = \text{Re} \left[-\frac{i\omega}{g} \phi(x, y) e^{-i\omega t} \right]. \quad (3)$$

Details of the multiple-scattering method, using Fourier-Bessel expansions, are given in Ref. 10. The transmittance of the waves is defined as $|\eta_{\text{trans}}/\eta_{\text{inc}}|^2$, where η_{trans} and η_{inc} represent the amplitude of transmitted and incident waves, respectively. The transmission spectra of water waves propagating through 2D graphitic and triangular structures are calculated numerically using the same parameters as in the experiments.

Transmittance of water waves through artificial crystals is measured in a small water tank (1000 mm × 400 mm × 250 mm) in the laboratory. The schematic diagram of our experimental setup, shown in Fig. 1, consists of two parts: one is the wave generation part and the other is the detection part. Water waves are generated electrically by exploiting the phenomenon of electrocapillarity of fluid, wherein the fluid rises toward higher electric fields. In our experiment a sinusoidally varying voltage, of amplitude 75 V, is applied between the bottom of the water tank and a razor blade situated right above the water surface within a distance of about 0.2 mm. One can assume that the amplitude of the water wave is much smaller than the wavelength and the applied electric field is appreciable only in a small region Δx . In particular, with a sinusoidal voltage $V_0 \cos \omega t$, the electric

^{a)}Electronic mail: hypark@kaist.ac.kr

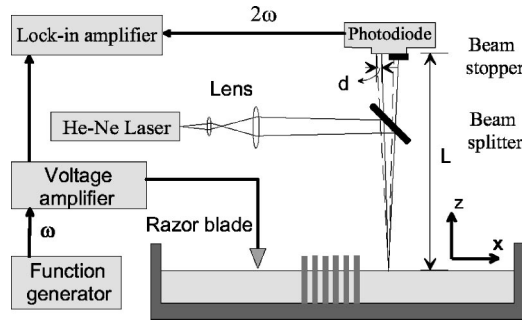


FIG. 1. Schematic diagram of experimental setup. The size of the water tank is 1000 mm \times 400 mm \times 250 mm.

field can be expressed as $\mathbf{g}(x, z)V_0 \cos \omega t$ where $\mathbf{g}(x, z)$ is a geometric factor. Thus, the force F acting on the water surface is

$$F = \frac{1}{16\pi} \frac{\epsilon_0(\epsilon_1 - \epsilon_0)}{\epsilon_0} V_0^2 (1 + \cos 2\omega t) \int_{\Delta x} |\mathbf{g}(x, 0)|^2 dx, \quad (4)$$

where ϵ_0 and ϵ_1 are the dielectric constants of air and water, respectively.¹¹ This force generates water waves whose frequency is twice that of the applied voltage. The amplitude of transmitted wave is obtained by measuring the deflection of a He-Ne laser beam reflected from the water surface, which acts like a rocking mirror. The elevation of the water wave, η , is related to the deflection angle θ of the laser beam by

$$\theta = 2k\eta \sin(kx - \omega t + \delta). \quad (5)$$

Under the assumption of small amplitude waves, η can be written as $\eta = (1/4k)(d/L)$, where L is the distance of the detector from the water surface, and d is the displacement of the beam on the detector. Since d is much smaller than the beam size, the signal detected by the half-sheltered photodiode is directly proportional to d and in turn, to the height of the water surface at a given position and wave number k . Using a lock-in amplifier, we can measure the amplitude of water waves at a given frequency. The relative transmittance is obtained by normalizing the amplitude of waves transmitted through the structures with that measured without the structures. In this detection method, it is obvious that the diameter of the laser beam must be smaller than $\lambda/2$ in order to be sensitive to the wave of wavelength λ . Thus the shortest detectable wavelength is limited by the beam size.

Artificial crystals used in this study consist of a finite 2D periodic array of vertical cylinders with a distance of $a = 19.6$ mm between the nearest cylinders. The cylinders of radius $r = 5$ mm, made of acrylic, are fixed at the bottom of the water tank ($h = 6$ mm). As shown in the insets of Figs. 2 and 3, 2D graphitic lattices and triangular lattices were setup for the experiments, in which Γ , P , and Q are the symmetry points in the first Brillouin zone of the corresponding structures.¹² In the graphitic lattice structure along the $\Gamma-P$ direction there are 100 cylinders with the number of layers of hexagons $N_L = 4.5$. Another graphitic structure used consists of 96 cylinders for the propagation along the $\Gamma-Q$ direction ($N_L = 4$). The filling fraction, f_{gr} , is 0.157 for both structures. In the triangular lattice structures, with $f_{tr} = 0.235$, there are 145 cylinders ($N_L = 4.5$) for the $\Gamma-Q$ and 153 cylinders ($N_L = 4$) for the $\Gamma-P$ direction, respectively.

Transmission spectra of water waves passing through the graphitic structures are shown in Fig. 2 for the frequency

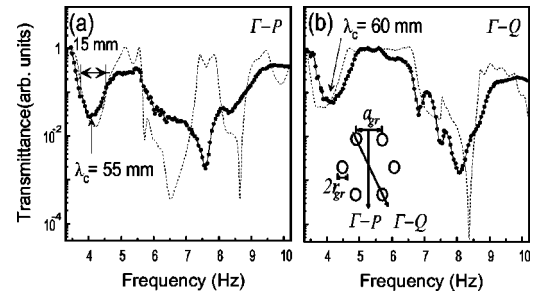


FIG. 2. Transmission spectra of water waves through the graphitic lattice structures; (a) the $\Gamma-P$ direction and (b) the $\Gamma-Q$ direction. The radius of the cylinder r_{gr} is 5 mm and the distance between the closest cylinders a_{gr} is 19.6 mm with the filling fraction $f_{gr} = 0.157$. Closed circles denote the measured data and dashed lines the numerical calculations. The center wavelength of the first band gap λ_c is 55 mm (60 mm) for the $\Gamma-P$ ($\Gamma-Q$) direction and the gap width is 15 mm.

range of 3–10 Hz. One can easily identify the WWBGs. The center of the first band gap exists, in each case, at around 4 Hz corresponding to a wavelength $\lambda_c = 55$ mm for the $\Gamma-P$ and 60 mm for the $\Gamma-Q$ direction, respectively. The widths of WWBGs along the two directions are nearly equal and about 15 mm. Notice that the lowest transmittance is of the order of 10^{-2} , which is much larger than in conventional photonic band gaps. This is attributed to the smaller number of unit cell layers in our setup. However the experimental data and the numerical calculations show fairly good agreement on the whole, especially in the first gap region; there is quite a discrepancy in both the position and size of the second band gap along the $\Gamma-P$ direction [Fig. 2(a)].

Transmission spectra for the triangular structures are shown in Fig. 3. Along the $\Gamma-Q$ direction the position of the experimentally determined band gap, with wider and shallower shape, is shifted a bit toward higher frequency region as compared with the simulation results. The gap is centered at $\lambda_c = 30$ mm and the gap width is about 15 mm. Comparing this with the first gaps of graphitic structures, which have similar spatial parameters, the widths of gaps are seen to be nearly the same, but the gap depths are larger by an order of magnitude ($T \sim 10^{-3}$) and the center wavelength of the gap is shorter in the triangular case by about half. In the $\Gamma-P$ direction of the triangular structures [Fig. 3(b)], the agreement between the experiment and theory is much worse than in the other three cases; the measured band gap seems to be broader and shallower than the simulation results, especially at higher frequencies. Presumably, this difference might have been caused by the imperfections in the periodic structures.

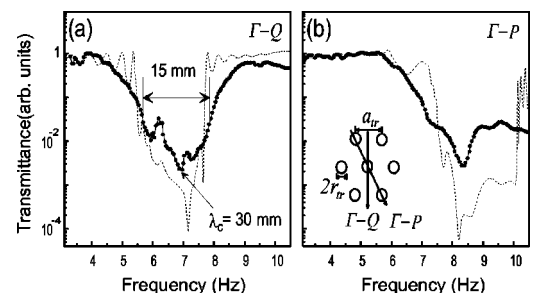


FIG. 3. Transmission spectra for triangular lattice structures; (a) the $\Gamma-Q$ direction and (b) the $\Gamma-P$ direction with $r_{tr} = 5$ mm, $a_{tr} = 19.6$ mm, and $f_{tr} = 0.235$. Closed circles represent the measured data and dashed lines the numerical calculations. The center wavelength of the first band gap λ_c is 30 mm for the $\Gamma-Q$ direction with the gap width of about 15 mm.

As they generally make the band gaps broader and shallower in all cases, even a small amount of structural imperfection may destroy the boundary between two band gaps, leading to a single wide gap. The higher frequency edge of this gap was unattainable as the wavelength at higher frequencies is too short to carry out the experiment. Also at higher frequencies the measured transmittance tends to be lower than the simulated values, probably due to the increased damping of the water waves.

In view of the results obtained so far, we consider the overall agreement between the experimental data and the numerical calculations to be satisfactory. If the transmittance of the waves becomes less than 10^{-2} , one may consider water waves to be practically blocked by the artificial crystals. If we view the transmittance spectra shown in Figs. 2 and 3 in this sense, the experiment and the theory are seen to be in good agreement with each other.

In this letter, we have demonstrated the existence of WWBGs in finite 2D periodic graphitic and triangular structures composed of an array of vertical cylinders which extend from the base of the water tank to the air above the water surface. The experimentally measured transmittance spectra agree fairly well with the numerical simulations based on the multiple scattering method. In our experiment, the center wavelengths of WWBGs are $\lambda_c=55$ and 60 mm for the graphitic structures and 30 mm for the triangular structures. The widths of WWBGs are about 15 mm. The first band gaps of the graphitic structures occur at longer wavelengths and at lower filling fraction compared with the triangular structures of the same spatial parameters, suggest-

ing that the graphitic lattice would be a better structure for coastal protection.⁹ For example, coastal water waves, with a period of the order of a few seconds, can be stopped by graphitic lattice structures whose lattice constant is about 10 m. Therefore, we suggest that the 2D periodic structures consisting of vertical cylinders, either filled or of shell-type, are a better eco-friendly option for coastal protection, since they allow water to flow freely, while curtailing the propagation of water waves at the same time.

This work was supported by the National Research Laboratory Project of Korea and also by Grant No. R04-2002-000-00176-0 from the Basic Research Program of the Korea Science and Engineering Foundation.

¹E. Yablonovitch, *Phys. Rev. Lett.* **58**, 2059 (1987).

²S. John, *Phys. Rev. Lett.* **58**, 2486 (1987).

³M. S. Kushwaha, and B. Djafari-Rouhani, *J. Sound Vib.* **218**, 697 (1999).

⁴C. S. Kee, J. E. Kim, H. Y. Park, K. J. Chang, and H. Lim, *J. Appl. Phys.* **87**, 1593 (2000).

⁵A. D. Heathershaw, *Nature (London)* **296**, 343 (1982); J. T. Kirby and R. A. Dalrymple, *J. Fluid Mech.* **133**, 47 (1983).

⁶T. Chou, *J. Fluid Mech.* **369**, 333 (1998).

⁷P. Mciver, *J. Fluid Mech.* **424**, 101 (2000).

⁸X. Hu, Y. Shen, X. Liu, R. Fu, J. Zi, X. Jiang, and S. Feng, *Phys. Rev. E* **68**, 037301 (2003).

⁹Y.-K. Ha, J. E. Kim, H. Y. Park, and I. W. Lee, *Appl. Phys. Lett.* **81**, 1341 (2002).

¹⁰C. M. Linton and D. V. Evans, *J. Fluid Mech.* **215**, 549 (1990), and references in Ref. 9.

¹¹C. H. Sohl, K. Miyano, and J. B. Ketterson, *Rev. Sci. Instrum.* **49**, 1464 (1978).

¹²D. Cassagne, C. Jouanim, and D. Bertho, *Phys. Rev. B* **53**, 7134 (1996).